© 2014. Published by The Company of Biologists Ltd | Journal of Cell Science (2014) 127, 4483–4493 doi:10.1242/jcs.154930

RESEARCH ARTICLE

AIMP1 negatively regulates adipogenesis by inhibiting PPARγ

Jong Hyun Kim[1], Jung Ho Lee[2], Min Chul Park[1], Ina Yoon[1], Kibom Kim[1], Minji Lee[3], Hueng-Sik Choi[4], Jung Min Han[3,5,*] and Sunghoon Kim[1,2,6,*]

ABSTRACT

Adipogenesis is known to be controlled by the concerted actions of transcription factors and co-regulators. However, little is known about the mechanism of regulation of the transcription factors that control adipogenesis. In addition, the adipogenic roles of translational factors remain unclear. Here, we show that aminoacyl tRNA synthetase-interacting multifunctional protein 1 (AIMP1, also known as p43), an auxiliary factor that is associated with a macromolecular tRNA synthetase complex, negatively regulates adipogenesis through a direct interaction with the DNA-binding domain of peroxisome proliferator-activated receptor γ (PPARγ). We found that AIMP1 expression increases during adipocyte differentiation. Adipogenesis is augmented in AIMP1-deficient cells, as compared with control cells. AIMP1 exhibits high affinity for active PPARγ and interacts with the DNA-binding domain of PPARγ, thereby inhibiting its transcriptional activity. Thus, AIMP1 appears to function as a novel inhibitor of PPARγ that regulates adipocyte differentiation by preventing the transcriptional activation of PPARγ.

KEY WORDS: AIMP1, PPARγ, Adipogenesis, tRNA synthetase

INTRODUCTION

Aminoacyl-tRNA synthetases (ARSs) catalyze the ligation of a specific amino acid to its cognate tRNA using ATP, thereby ensuring faithful translation of the genetic code (Kim et al., 2011; Park et al., 2008). Aminoacyl-tRNA synthetase-interacting multifunctional protein 1 (AIMP1, also known as p43) has been identified as a non-enzymatic factor associated with the ARS complex, which consists of nine different enzymes (Çirakoğlu et al., 1985; Mirande et al., 1982; Norcum, 1989) and three non-enzymatic factors (Lee et al., 2004; Quevillon and Mirande, 1996; Quevillon et al., 1997; Quevillon et al., 1999). AIMP1 regulates the catalytic reaction of arginyl-tRNA synthetase (RRS), as well as the stability of the ARS complex, through protein–protein interaction (Park et al., 1999; Han et al., 2006). AIMP1 is associated with various physiological functions, including angiogenesis (Park, et al., 2002b), wound healing (Park et al., 2005) and autoimmunity (Han et al., 2007). It is also highly enriched in pancreatic α cells, from which it is secreted to maintain glucose homeostasis (Park et al., 2006).

Adipose tissue is one the most dynamic types of tissue in the body and is a crucial exchange center for complex energy transactions (Galic et al., 2010; Haque and Garg, 2004; Rosen and Spiegelman, 2006). However, an imbalance between energy intake and expenditure leads to metabolic disorders (Méndez-Sánchez et al., 2006; Kalra and Kalra, 2002). Adipogenesis, the cell differentiation mechanism by which preadipocytes become adipocytes, entails complex processes and steps, such as commitment of preadipocytes, growth arrest, clonal expansion, terminal differentiation and maturation of adipocytes (Grimaldi, 2001; Ntambi and Young-Cheul, 2000). The terminal stages of adipogenic differentiation have been extensively studied using immortalized preadipocyte lines (Couture et al., 2009; Han et al., 2012).

Adipogenesis is governed by a multifaceted transcriptional regulatory cascade. Three classes of transcription factors are known to influence adipogenesis directly. These include peroxisome proliferator-activated receptor gamma (PPARγ), members of the CCAAT/enhancer-binding protein families (C/EBPs) and members of the basic helix-loop-helix family (ADD1 and SREBP1c) (Rosen et al., 2000). PPARγ is a member of the nuclear-receptor family of ligand-activated transcription factors that is highly expressed in white adipose tissues, where it is required for adipocyte differentiation (Koppen and Kalkhoven, 2010; Tontonoz and Spiegelman, 2008). Accumulating evidence has suggested that no factor is capable of guiding cells to differentiate into adipocytes in the absence of PPARγ, whereas forced expression of PPARγ is sufficient to induce the differentiation of fibroblasts into adipocytes (Rosen et al., 1999; Tontonoz et al., 1994). PPARγ activates the promoter of the gene encoding C/EBPα, and vice versa, creating a positive-feedback loop. In addition, PPARγ and C/EBPα induce the expression of genes that are involved in insulin sensitivity, lipogenesis and lipolysis (Lefterova et al., 2008).

The sirtuin SIRT2 inhibits PPARγ indirectly by reducing the levels of acetylation of forkhead box O1 (FOXO1). This leads to an increase in the nuclear localization of FOXO1, which subsequently represses the transcription of the gene encoding PPARγ (Jing et al., 2007). Another sirtuin, SIRT1, impairs adipogenesis by directly acting as a PPARγ co-repressor (Picard et al., 2004). The nuclear co-repressor (NCoR1) and silencing mediator of retinoid and thyroid hormone (SMRT, also known as NCoR2) proteins have been identified as nuclear receptor co-repressors that control the transcriptional activity of PPARγ (Cohen et al., 1998; Yu et al., 2005). NCoR and SMRT recruit a complex exhibiting histone deacetylase activity to repress the transcription of target genes. In addition, NCoR and SMRT are recruited by other nuclear receptors and interact with nuclear

[1]Medicinal Bioconvergence Research Center, Seoul National University, Seoul 151-742, South Korea. [2]College of Pharmacy, Seoul National University, Seoul 151-742, South Korea. [3]Department of Integrated OMICS for Biomedical Science, Yonsei University, Seoul 120-749, South Korea. [4]National Creative Research Initiatives Center for Nuclear Receptor Signals, School of Biological Sciences and Technology, Chonnam National University, Gwangju 500-757, South Korea. [5]College of Pharmacy, Yonsei University, Incheon 406-840, South Korea. [6]Department of Molecular Medicine and Biopharmaceutical Sciences, Seoul National University, Seoul 151-742, South Korea.

*Authors for correspondence (jhan74@yonsei.ac.kr; sungkim@snu.ac.kr)

Received 10 April 2014; Accepted 4 August 2014

Journal of Cell Science (2014) 127, 4483–4493 doi:10.1242/jcs.154930

receptor co-repressors in a ligand-dependent manner (Cohen 2006; Yu et al., 2005).

Although PPARγ is known as an important factor playing a role in the strict control of adipogenesis, little is known about the regulation of PPARγ activity through protein–protein interaction. In this study, we show the molecular mechanisms by which AIMP1 regulates adipocyte differentiation through the catalytic inhibition of PPARγ.

RESULTS

Dynamic alteration of AIMP1 expression during the differentiation of 3T3-L1 preadipocytes

During adipocyte differentiation, the gene expression profile changes markedly. Although the adipogenic role attributed to the white adipose tissue (WAT) is energy storage, protein synthesis is an energy-consuming process (Trayhurn and Beattie, 2001; Rosen et al., 2000). Here, we specifically investigated the changes in the expression of genes encoding tRNA synthetases and their associated factors that are involved in protein synthesis during adipogenesis. Whereas the expression of genes encoding adipogenic markers, such as lipoprotein lipase (LPL), RXRα and sterol regulatory element-binding transcription factor 1 (SREBP1), was increased during the differentiation of 3T3-L1 cells, the expression of *SIRT1* was decreased, as was the expression of genes encoding ten different tRNA synthetases – glutamyl-prolyl-tRNA synthetase (EPRS), methionyl-tRNA synthetase (MRS), isoleucyl-tRNA synthetase (IRS), valyl-tRNA synthesis (VRS), tryptophanyl-tRNA synthetase (WRS), aspartyl-tRNA synthetase (DRS), arginyl-tRNA synthetase (RRS), leucyl-tRNA synthetase (LRS), glycyl-tRNA synthetase (GRS) and histidyl-tRNA synthetase (HRS) – and that of genes encoding two AIMPs, AIMP2 and AIMP3 (Fig. 1A). These findings suggest that aminoacyl-tRNA synthesis and ATP consumption is decreased during adipogenesis. However, the expression pattern of the gene encoding AIMP1 was different from that of genes encoding AIMP2 and AIMP3. *AIMP1* mRNA expression peaked at 4–6 days after differentiation (Fig. 1A,B). Although the protein expression of AIMP1 was slightly delayed,

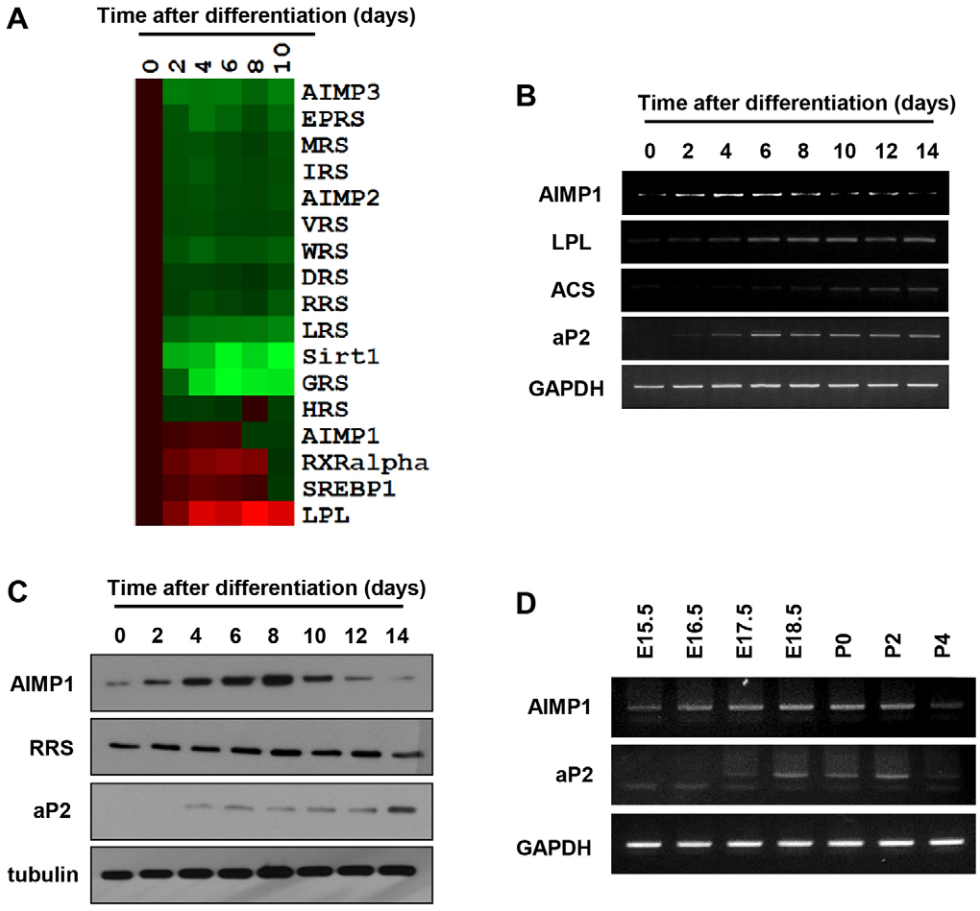

Fig. 1. Expression of genes encoding ARSs and AIMPs during the differentiation of 3T3-L1 preadipocytes. (A) A heat map of mRNA expression in 3T3-L1 cells during adipogenesis. 3T3-L1 preadipocytes were differentiated and harvested every 2 days. The initial day of differentiation was designated as day 0, and changes in expression are shown relative to expression on day 0. Quantification of mRNA expression is represented by a heat map on a 10% scale, from green to red. (B) Total RNA was extracted from cell lysates and quantitative RT-PCR was performed using specific primers. As a control, *GAPDH* mRNA levels were also quantified from the same RNA samples by RT-PCR. The level of each gene transcript was normalized to that of *GAPDH*. The data shown are representative of three independent experiments. (C) 3T3-L1 preadipocytes were differentiated, harvested every 2 days and lysed with lysis buffer, and the lysate proteins were then separated by SDS-PAGE and immunoblotted using the indicated antibodies. The data shown are representative of three independent experiments. (D) Total RNA was extracted from C57BL/6 mouse embryos and animals at postnatal days 0, 2 and 4, and quantitative RT-PCR was performed using specific primers. As a control, *GAPDH* mRNA levels were also quantified from the same RNA samples by RT-PCR. The level of each gene transcript was normalized to that of *GAPDH*. The data shown are representative of three independent experiments.

Journal of Cell Science (2014) 127, 4483–4493 doi:10.1242/jcs.154930

peaking only at 6–8 days after differentiation, the expression of RRS, which is a binding partner of AIMP1 within the multi-tRNA synthetase complex, remained unchanged during adipocyte differentiation (Fig. 1C). In addition, we also examined *AIMP1* expression during adipose tissue development in mice. RT-PCR analysis was performed on RNA isolated from the developing WAT fractions at pre- and postnatal time-points (Birsoy et al., 2011). As shown in Fig. 1D, *AIMP1* mRNA was expressed at relatively low levels in early embryonic (E15.5 and E16.5) and postnatal time-points (P2 and P4), but its expression was greatly increased at E18.5 and P0 (Fig. 1D), consistent with *AIMP1* expression in 3T3-L1 cells (Fig. 1B). Taken together, these results suggest that the stoichiometry of AIMP1 to RRS is altered and that AIMP1 has a novel function during adipocyte differentiation.

Nuclear localization of AIMP1 during adipogenesis

To examine the function of AIMP1 during adipocyte differentiation, we first analyzed the subcellular localization of AIMP1. As shown in Fig. 2A, a portion of AIMP1 was clearly localized in the nucleus in differentiated 3T3-L1 adipocytes but not in preadipocytes. Although AIMP1 was mainly expressed in the cytoplasm in 3T3-L1 preadipocytes, the AIMP1 level was increased and the protein translocated to the nucleus in mature adipocyte, where it colocalized with propidium iodide staining. Biochemical fractionation also showed an increase in AIMP1 in both the cytoplasm and nucleus during adipogenesis (Fig. 2B).

To clarify the region of AIMP1 responsible for its nuclear translocation, we generated two truncated mutants of AIMP1 – a C-terminally truncated version (amino acids 1–146) and an N-terminally truncated mutant (amino acids 146–312). As shown in

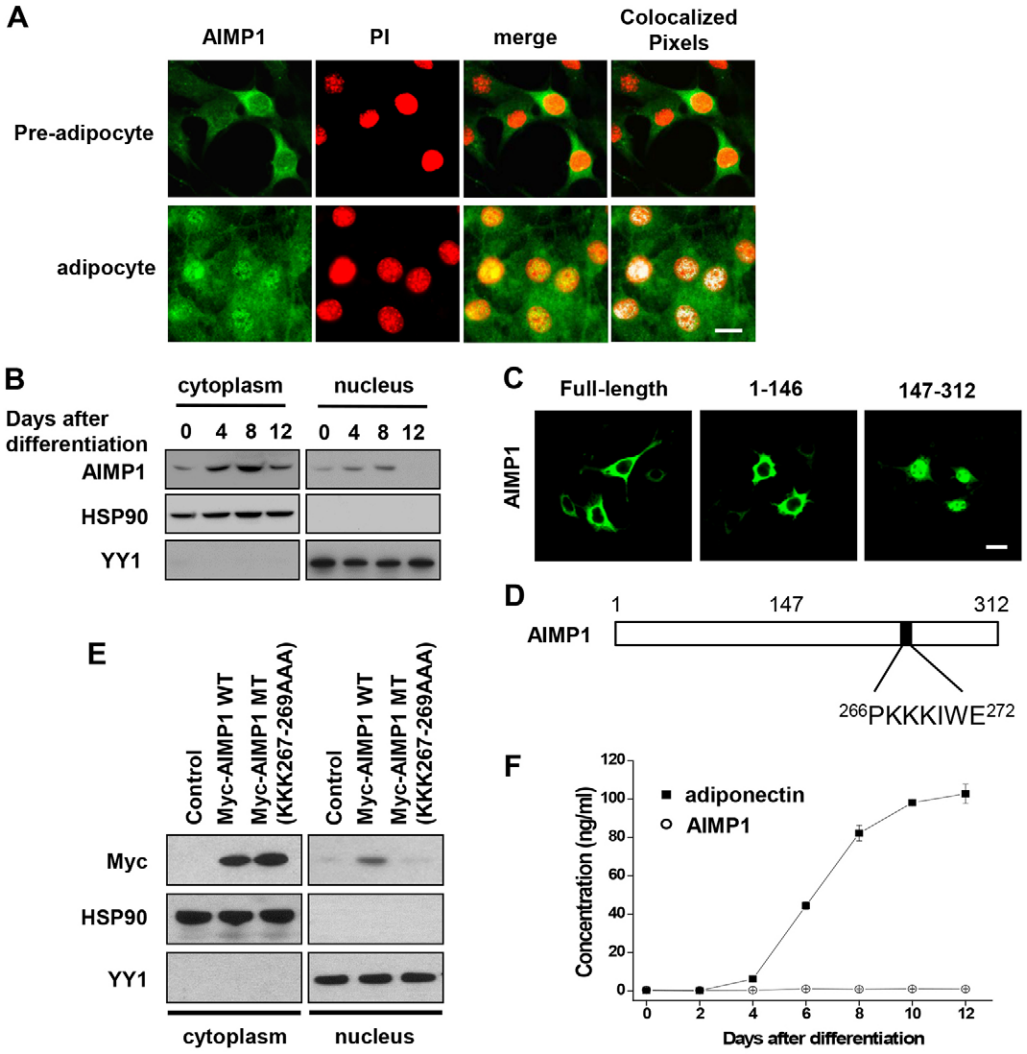

Fig. 2. AIMP1 translocates to the nucleus in 3T3-L1 adipocytes. (A) Immunofluorescence assays, using anti-AIMP1 antibodies (green), were performed in 3T3-L1 preadipocytes and 3T3-L1 adipocytes. Propidium iodide (PI) was used as a nuclear stain. Scale bar: 20 μm. (B) The cytosol and nucleus of 3T3-L1 adipocytes were fractionated at the indicated days, as described in Materials and Methods. Cell lysates were separated by SDS-PAGE and immunoblotted using antibodies against AIMP1, YY1 (a nuclear marker) and HSP90 (a cytoplasmic marker). (C) 3T3-L1 preadipocytes were transfected with GFP–AIMP1 (full length), GFP-tagged C-terminally truncated mutant (amino acids 1–146) or GFP-tagged N-terminally truncated mutant (amino acids 147–312). Cells were visualized by using fluorescence microscopy. Scale bar: 20 μm. (D) AIMP1 primary sequence showing the candidate nuclear targeting motif. (E) The cytoplasm and nucleus were fractionated after transfection with wild-type Myc–AIMP1 (WT) or the Myc-AIMP1 mutant (MT, KKK267-269AAA), as described in Materials and Methods. Cell lysates were separated by SDS-PAGE and immunoblotted using antibodies against Myc, YY1 and HSP90. (F) 3T3-L1 preadipocytes were differentiated; thereafter, the culture medium was harvested at the indicated days. The amount of secreted adiponectin and AIMP1 was quantified using specific ELISA kits. The data are shown as the mean±s.d. (n=3).

Journal of Cell Science (2014) 127, 4483–4493 doi:10.1242/jcs.154930

Fig. 2C, the N-terminally truncated mutant was mainly located in the nucleus, whereas the C-terminally truncated mutant still showed cytoplasmic staining (Fig. 2C). To identify the sequence of AIMP1 responsible for its nuclear translocation, we searched for a candidate nuclear localization signal (NLS) in the AIMP1 C-terminus using bioinformatic tools and found one candidate NLS – triple lysine residues (^{267}KKK^{269}) in the C-terminus of AIMP1 (Fig. 2D). When these triple lysine residues were mutated to triple alanine residues, the mutated AIMP1 (KKK267-269AAA) could no longer translocate to the nucleus (Fig. 2E). These results indicate that AIMP1 translocates to the nucleus in a manner dependent on its NLS during adipocyte differentiation.

Because AIMP1 can function as a secreted factor (Park et al., 2002a; Park et al., 2005; Park et al., 2006; Han et al., 2010), we examined whether AIMP1 is secreted during adipogenesis. Although adiponectin, an adipokine produced and secreted by adipocytes, was detected in the culture medium of adipocytes, AIMP1 was not detected (Fig. 2F). Taken together, these results also suggest that AIMP1 has a novel function in the nucleus during adipogenesis.

Negative regulation of adipogenesis by AIMP1

To investigate the effect of AIMP1 on adipogenesis, we used AIMP1-deficient mouse embryonic fibroblasts (MEFs) and 3T3-L1 preadipocytes that had been transfected with *AIMP1*-specific siRNA. The mRNA expression of adipogenic genes, such as those encoding acyl-CoA synthetase (ACS), fatty acid synthase (FAS) and SREBP-1, was elevated in AIMP1-deficient MEFs compared with that in wild-type cells by 8 days after differentiation (Fig. 3A). The same results were observed in the *AIMP1*-siRNA-transfected 3T3-L1 cells (Fig. 3B).

When the accumulation of intracellular lipids was monitored by Oil Red O staining, the intensity of Oil Red O staining was increased in AIMP1-deficient MEFs and in AIMP1-downregulated cells (Fig. 3C,D). In addition, the triglyceride content was elevated in AIMP1-deficient MEFs and in AIMP1-downregulated cells during adipogenesis (Fig. 3E,F). Expression of adipogenic proteins [aP2 (also known as FABP4), RXRα and C/EBPα] rapidly increased in AIMP1-deficient MEFs and in AIMP1-downregulated cells, as compared with that of control cells (Fig. 3G,H).

To examine whether AIMP1 overexpression suppresses adipogenesis, we generated cell lines with inducible *AIMP1*, which was overexpressed in the absence of tetracycline (tet). As shown in Fig. 4A, the expression of the adipogenic markers aP2 and C/EBPα was decreased by the induction of *AIMP1* expression during differentiation. Accumulation of intracellular lipid droplets

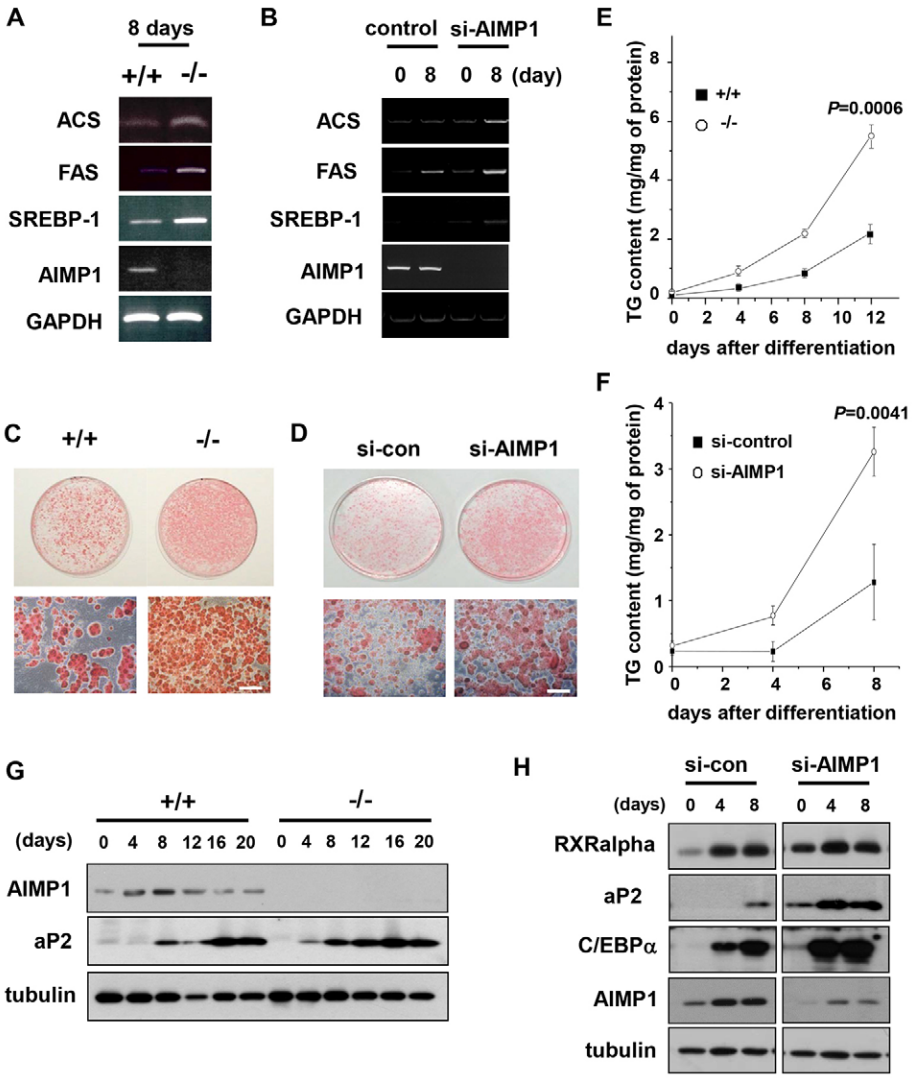

Fig. 3. Silencing of AIMP1 promotes adipogenesis. (A) AIMP1$^{+/+}$ and AIMP1$^{-/-}$ MEFs were differentiated as described in Materials and Methods. At day 8 after differentiation, total RNA was extracted from AIMP1$^{+/+}$ and AIMP1$^{-/-}$ MEFs. RT-PCR was performed using specific primers. (B) 3T3-L1 preadipocytes were transfected with siRNA directed against *AIMP1* (si-AIMP1) or with a control siRNA, differentiated and harvested at the indicated day. RT-PCR was performed using specific primers. (C) AIMP1$^{+/+}$ and AIMP1$^{-/-}$ MEFs were differentiated and stained with Oil Red O staining solution. High-magnification images are shown in the lower panels. (D) 3T3-L1 preadipocytes were transfected with siRNA directed against AIMP1 or with a control siRNA (si-con), differentiated and stained with Oil Red O staining solution. High-magnification images are shown in the lower panels. Scale bars: 100 μm. (E) Triglyceride (TG) contents were measured in AIMP1$^{+/+}$ and AIMP1$^{-/-}$ MEFs during differentiation. P=0.0006 at day 12. (F) 3T3-L1 preadipocytes were transfected with siRNA directed against *AIMP1* or with a control siRNA. During differentiation, triglyceride contents were measured at the indicated days. P=0.0041 at day 8. The data are shown as the mean±s.d. (n=3). (G) AIMP1$^{+/+}$ and AIMP1$^{-/-}$ MEFs were differentiated and harvested at the indicated days, and the lysates were immunoblotted using the indicated antibodies. (H) 3T3-L1 preadipocytes were transfected with siRNA directed against *AIMP1* or with a control siRNA and differentiated, and the lysates were immunoblotted using the indicated antibodies.

Journal of Cell Science (2014) 127, 4483–4493 doi:10.1242/jcs.154930

and triglyceride contents was suppressed in *AIMP1*-overexpressing cells, as shown by Oil Red O staining and triglyceride content assays (Fig. 4B,C). To examine the effect of the transient overexpression of *AIMP1* on adipogenesis, we generated an *AIMP1*-overexpressing adenovirus with which we infected 3T3-L1 preadipocytes. Expression of aP2 and C/EBPα during adipocyte differentiation was attenuated in cells infected with the *AIMP1*-adenovirus, compared with that of cells infected with the control *LacZ*-adenovirus (Fig. 4D). Furthermore, accumulation of intracellular lipid droplets and triglyceride content was suppressed in cells infected with the *AIMP1*-adenovirus compared with that of cells infected with the *LacZ*-adenovirus (Fig. 4E,F). Taken together, these results indicated that AIMP1 inhibits adipogenesis.

Negative effect of AIMP1 on adipogenesis *in vivo*

To validate the effect of AIMP1 on adipogenesis *in vivo*, we injected the *LacZ*- or *AIMP1*-adenovirus into mouse epididymal fat pads. The epididymal fat pads (which are WAT), liver and muscle tissues were removed from sacrificed mice, and the expression of *AIMP1* and adipogenic markers was analyzed. When adenoviruses expressing either *AIMP1* or *LacZ* were injected into the fat pads, the expression of AIMP1 in the liver and muscle tissues was not affected (Fig. 5A). However, in the epididymal fat pads, the expression of adipogenic marker proteins was changed significantly by *AIMP1*-adenovirus injection. Although the expression of lysyl-tRNA synthetase (KRS) was not changed by AIMP1 overexpression, the expression of FAS and aP2 was substantially reduced in *AIMP1*-adenovirus-injected epididymal fat pads compared with that of *LacZ*-adenovirus-injected epididymal fat pads (Fig. 5A, left and right panel in WAT but not liver or muscle). Although the body weight of the mice and the plasma levels of AIMP1 were not changed by adenoviral infection of WAT, plasma TNFα, adiponectin and triglyceride contents were decreased in mice that had been infected with the *AIMP1*-adenovirus, as compared with those that had been infected with the *LacZ*-adenovirus (Fig. 5B–F). Conversely, both plasma non-esterified fatty acid (NEFA) and insulin levels were increased in mice infected with the *AIMP1*-adenovirus (Fig. 5G,H).

Next, we performed an intra-peritoneal glucose tolerance test (IPGTT) to compare the glucose sensitivity of *LacZ*-adenovirus-infected mice and *AIMP1*-adenovirus-infected mice. Overexpression of AIMP1 in WAT resulted in slower removal of blood glucose than did overexpression of LacZ in WAT (Fig. 5I). These results further indicate that AIMP1 is a negative regulator of adipogenesis *in vivo*.

Negative regulation of PPARγ by AIMP1

To elucidate how AIMP1 regulates adipogenesis, we first examined the effect of AIMP1 on the transcriptional activities

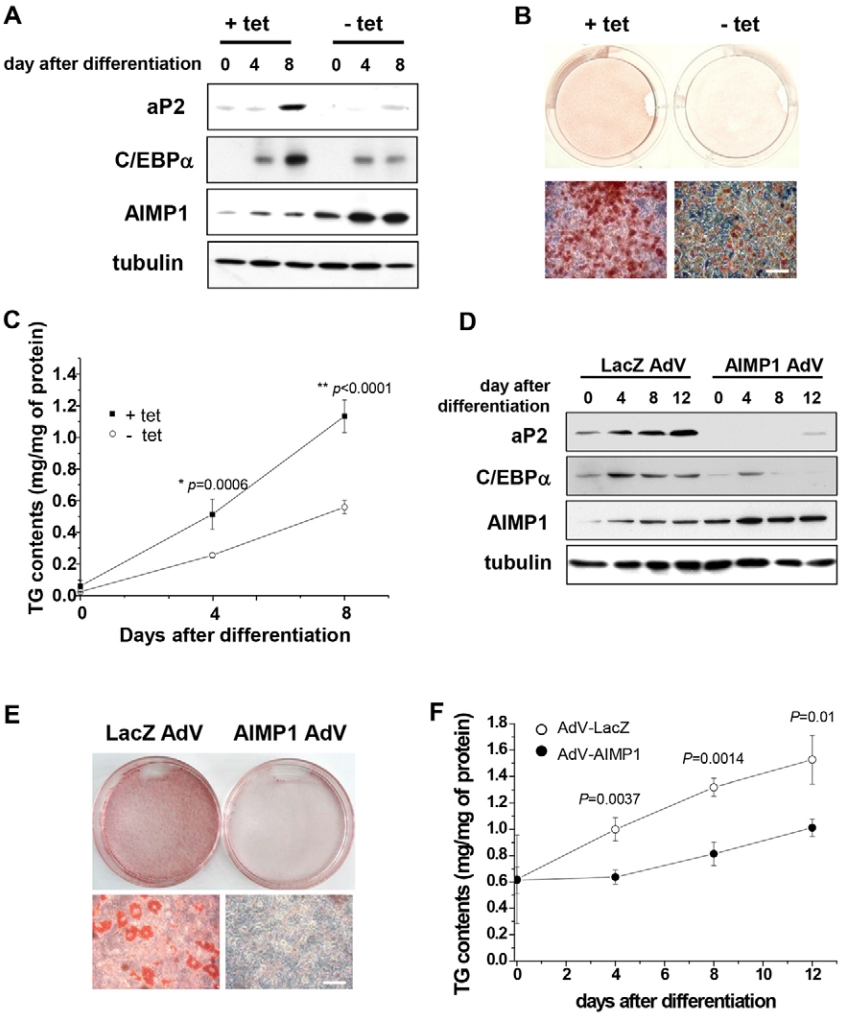

Fig. 4. Overexpression of AIMP1 delays adipogenesis. (A) AIMP1-inducible cell lines, which were cultured in the presence or absence of tetracycline (tet), were differentiated, harvested at days 0, 4 or 8, and immunoblotted using the indicated antibodies. (B) AIMP1-inducible cell lines were differentiated and then stained with Oil Red O solution. High-magnification images are shown in the lower panels. Scale bars: 100 μm. (C) Triglyceride (TG) contents in AIMP1-inducible cell lines that had been cultured in the presence or absence of tet were measured during differentiation. $P=0.0006$ at day 4; $P<0.0001$ at day 8. (D) 3T3-L1 preadipocytes were infected with adenovirus (AdV)-LacZ or AdV-AIMP1, harvested at 0, 4, 8 and 12 days after differentiation, and immunoblotted using the indicated antibodies. (E) 3T3-L1 preadipocytes were infected with AdV-LacZ or AdV-AIMP1. After differentiation, 3T3-L1 adipocytes were stained with Oil Red O solution. High-magnification images are shown in the lower panels. Scale bars: 100 μm. (F) 3T3-L1 preadipocytes were infected with AdV-LacZ or AdV-AIMP1. After differentiation, triglyceride contents were measured. $P=0.0037$ at day 4, $P=0.0014$ at day 8, $P<0.01$ at day 12. Data in C,F are shown as the mean±s.d. ($n=3$).

Journal of Cell Science (2014) 127, 4483–4493 doi:10.1242/jcs.154930

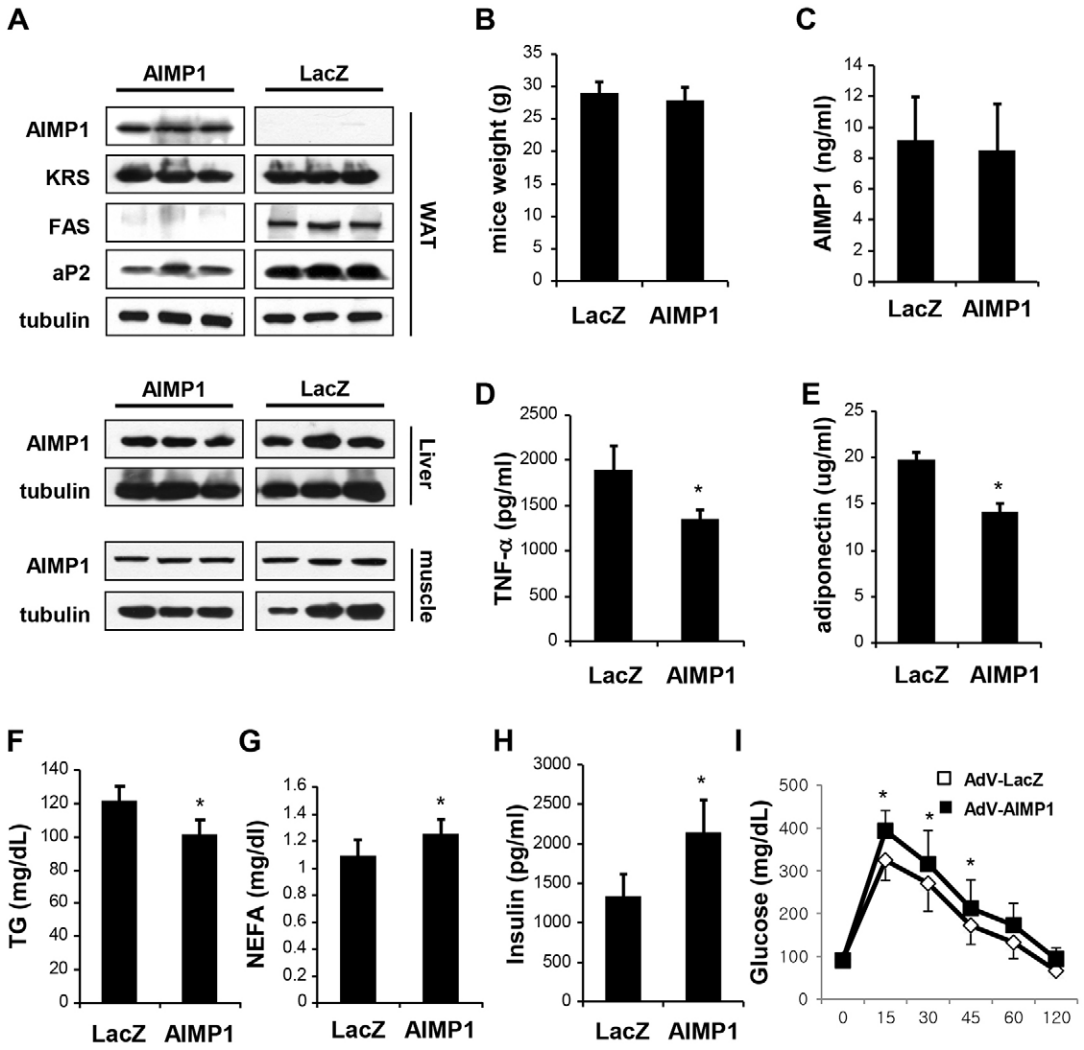

Fig. 5. The effects of AIMP1 on adipogenesis *in vivo*. The mouse fat pad was injected with adenovirus (AdV)-LacZ or AdV-AIMP1 as described in Materials and Methods. (A) The white adipose tissue (WAT), liver and muscle were extracted from mice, lysed with lysis buffer, separated by SDS-PAGE and immunoblotted with the indicated antibodies. Body weight (B), blood AIMP1 levels (C), serum TNFα levels (D), serum adiponectin levels (E), serum triglyceride (TG) levels (F), serum NEFA levels (G) and serum insulin levels (H) of AdV-LacZ mice and AdV-AIMP1 mice were measured on day 3 after adenoviral administration. (I) Glucose-tolerance test was performed on day 3. Data are presented as the mean and s.d. (n=6 per group); *P<0.05 (unpaired Student's t-test).

of PPARγ, SREBP1c and ERRγ, which are the major transcription factors involved in adipogenesis (Kim et al., 1998; Spiegelman 1998; Kubo et al., 2009). Although AIMP1 had no effect on the transcriptional activities of SREBP1c and ERRγ (supplementary material Fig. S1A,B), AIMP1 suppressed PPARγ transcriptional activity in a dose-dependent manner, as well as suppressing RXRα-induced PPARγ transcriptional activity (Fig. 6A,B). Because the AIMP1 mutant KKK267-269AAA cannot translocate to the nucleus (Fig. 2E), we investigated whether this mutant could regulate PPARγ transcriptional activity by using a luciferase assay in the absence or presence of rosiglitazone (a PPARγ agonist). The AIMP1 mutant did not suppress PPARγ transcriptional activity regardless of rosiglitazone, whereas wild-type AIMP1 suppressed the transcriptional activity of PPARγ under the same conditions (supplementary materials Fig. S1C). These results suggest that nuclear translocation of AIMP1 is important for negative regulation of PPARγ.

Next, we investigated the association between PPARγ and AIMP1. Endogenous AIMP1 interacted with PPARγ in 3T3-L1 adipocytes (Fig. 6C). To assess whether AIMP1 binds specifically to particular isoforms of PPAR, we overexpressed either GFP-tagged PPARγ or PPARδ in 293T cells that expressed Myc-tagged AIMP1. AIMP1 co-immunoprecipitated with GFP–PPARγ but not with GFP–PPARα (Fig. 6D). To identify the region of AIMP1 responsible for the interaction with PPARγ, several GFP-fusion constructs of PPARγ were generated. As shown in Fig. 6E, the full-length PPARγ (amino acids 1–475) interacted with AIMP1. Although GFP–PPARγ-D (the DNA-binding domain; amino acids 94–181) as well as GFP–PPARγ-DL (the DNA-binding domain+the ligand-binding domain; amino acids 94–475) also interacted with AIMP1, GFP–PPARγ-L (the ligand-binding domain alone; amino acids 281–475) did not interact with AIMP1 under the same conditions. This finding indicates that the DNA-binding domain of PPARγ is required for interaction with AIMP1.

We then examined whether the conformation of PPARγ affects AIMP1 binding. Purified PPARγ was incubated with GST alone or with GST–AIMP1 in the presence of GW9662 (a PPARγ

Journal of Cell Science (2014) 127, 4483–4493 doi:10.1242/jcs.154930

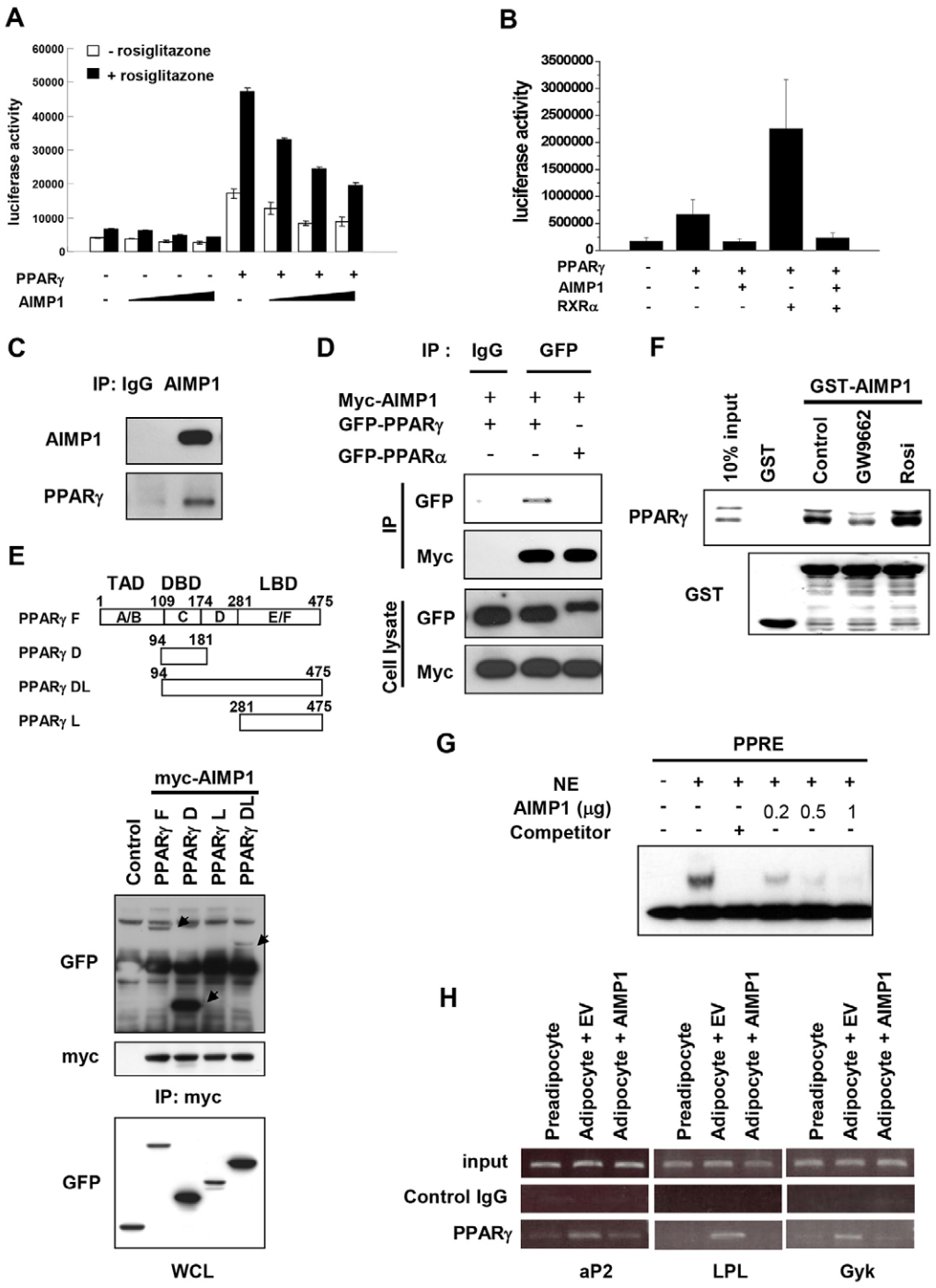

Fig. 6. See next page for legend.

antagonist) or rosiglitazone, followed by immunoblot analysis. Rosiglitazone but not GW9662 significantly increased the binding affinity of PPARγ for AIMP1 (Fig. 6F). Because AIMP1 interacted with the DNA-binding domain of PPARγ and suppressed its transcriptional activity, we investigated whether AIMP1 directly inhibits the binding of PPARγ to the peroxisome proliferator-activated receptor response element (PPRE) on the DNA. Purified AIMP1 was incubated with nuclear extracts of differentiated 3T3-L1 cells and a biotin-labeled PPRE. As shown in Fig. 6G, purified AIMP1 prevented the binding of PPARγ to PPRE in a dose-dependent manner. Chromatin immunoprecipitation (ChIP) assays were performed to confirm the effect of AIMP1 on PPARγ-binding to target genes, such as those encoding aP2, LPL and glycerol kinase (Gyk), in 3T3-L1 adipocytes. As shown in Fig. 6H, PPARγ dissociated from the promoter regions of the genes encoding aP2, LPL and Gyk in 3T3-L1 adipocytes infected with the *AIMP1*-adenovirus. These results indicate that AIMP1 negatively regulates the transcriptional activity of PPARγ by competing with the interaction between the PPARγ DNA-binding domain and the target gene.

Fig. 6. AIMP1 regulates PPARγ transcriptional activity through direct binding to PPARγ. (A) HEK293 cells were transfected with the indicated plasmids encoding PPARγ and AIMP1 (0, 1, 2, 5 μg) and with reporter plasmids, such as the PPARγ response element-luciferase construct (PPRE-tk-Luc). Cells were treated with the PPARγ agonist rosiglitazone (1 μM, 24 h) and harvested for the luciferase assays. The luciferase activity of PPARγ was measured in the presence or absence of rosiglitazone. Luciferase activity was normalized to β-gal activity. (B) HEK293 cells were transfected with the indicated plasmids encoding PPARγ, AIMP1 or RXRα. After transfection, cells were harvested for the luciferase assays. Luciferase activity was normalized to β-gal activity. Data are presented as the mean±s.d. (C) Differentiated 3T3-L1 adipocytes were harvested, lysed and immunoprecipitated (IP) using anti-AIMP1 antibodies or control IgG. PPARγ co-immunoprecipitated with AIMP1. (D) 293T cells that had been transfected with Myc–AIMP1 and either GFP–PPARγ or GFP–PPARα were harvested, lysed and immunoprecipitated using an anti-Myc antibody or IgG as a control. The immunoprecipitates were immunoblotted with the indicated antibodies. (E) Upper panel, schematic diagram of the individual fragments of PPARγ used in this study. Lower panels, HEK293 cells were transfected with Myc–AIMP1 and GFP–PPARγ constructs. Myc–AIMP1 co-immunoprecipitated with PPARγ-D and PPARγ-DL. WCL, whole cell lysate. (F) Cell lysates from 3T3-L1 cells treated with DMSO, GW9662 (1 μM, 24 h) or rosiglitazone (rosi, 1 μM, 24 h) were mixed with GST–AIMP1 (full length) and affinity precipitated using glutathione–Sepharose beads. Co-precipitation of PPARγ with GST–AIMP1 was assessed by immunoblotting with an anti-PPARγ antibody. (G) The endogenous PPARγ in nuclear extracts (NE) interacted with the PPARγ-response element (PPRE). Purified AIMP1 was added at the indicated dose and inhibited the binding of PPARγ in a dose-dependent manner. Competitor was used as a positive control for inhibition. (H) 3T3-L1 adipocytes were transfected with either control (EV) or AIMP1. Immuno-complexes were precipitated with control IgG or anti-PPARγ antibodies and PCR was performed using primers specific for the genes encoding aP2, LPL, and Gyk.

DISCUSSION

AIMP1 plays distinct roles in specific cell types and tissues. In our previous study, we found that secreted AIMP1 functions in the maintenance of glucose homeostasis by inducing glucagon secretion in the pancreas, thus inhibiting glucose uptake and glycogenolysis in the liver, and enhancing lipolysis in adipose tissue (Park et al., 2006). Genetic depletion of AIMP1 induces hypoglycemia *in vivo* (Park et al., 2006). Here, we showed that, in adipose tissues, AIMP1 negatively regulates PPARγ and adipogenesis.

AIMP1 overexpression in WAT can affect blood levels of TNFα, insulin, adiponectin, NEFA and triglyceride. Thus, to some extent, the metabolic phenotypes of AIMP1$^{-/-}$ mice might be due to intracellular AIMP1 depletion and activation of PPARγ activity. Interestingly, liver PPARγ contributes to hepatic steatosis (Gavrilova et al., 2003; Yu et al., 2003), and AIMP1$^{-/-}$ mice show a hepatic steatosis phenotype (data not shown), which might be caused by hepatic elevation of PPARγ activity.

During adipocyte differentiation, cells first undergo growth arrest, re-enter the cell cycle under the influence of differentiation inducers, undergo mitotic clonal expansion and, finally, exit the cell cycle to undergo terminal differentiation (Gao et al., 2013; Tang et al., 2003). During the early phase of adipocyte differentiation, AIMP1 levels increase; the protein then translocates to the nucleus, where it interacts with and inhibits the transcriptional activity of PPARγ (Fig. 2B; Fig. 6A). As shown in Fig. 1A, the mRNA level of *SIRT1*, a known repressor of PPARγ, was decreased during adipogenesis. Although *SIRT1* mRNA level was decreased, PPARγ activity was not always high, indicating that other repressors are needed for the fine control of PPARγ activity during adipogenesis. Here, we suggest that AIMP1 is a novel inhibitor of PPARγ activity and that the joint action of AIMP1 and SIRT1 in fine-tuning PPARγ activity might be required for the control of adipogenesis.

Moreover, FOXO1 and SIRT2 are known to inhibit adipogenesis through PPARγ inhibition. Adipogenesis is regulated by acetylation and deacetylation of FOXO1, which is mediated by SIRT2. SIRT2 decreases the acetylation levels of FOXO1, increasing its binding to PPARγ, which, in turn, inhibits the transcriptional activity of PPARγ (Jing et al., 2007). FOXO1 also interacts with PPARγ in a rosiglitazone-dependent manner, but the regions responsible for the binding of PPARγ to FOXO1 remain unclear (Wang and Tong, 2009). In this study, we showed that AIMP1 interacts with the DNA-binding domain of PPARγ in a rosiglitazone-dependent manner, although the upstream regulator of AIMP1 remains unknown.

In this study, we revealed a novel role of AIMP1 in adipogenesis. Our data suggest that, upon adipogenesis, AIMP1 is induced and translocates to the nucleus, where it binds to the DNA-binding domain of PPARγ and suppresses the transcription of PPARγ target genes. This work identified a translational factor, AIMP1, as a new key player in the control of adipogenesis and suggests a potential connection between translation in the cytosol and adipogenesis-related gene expression in the nucleus. The physiological interaction between AIMP1 and PPARγ revealed here also provides a novel pharmacological target in the treatment of metabolic syndromes such as obesity.

MATERIALS AND METHODS

Quantitative RT-PCR

Total RNA was isolated using TRIzol Reagent (Molecular Research Center, Cincinnati, OH), according to the manufacturer's instructions. Total RNA was quantified by absorbance at 260 nm, and the integrity of the RNA was checked using the 2100 Bioanalyzer (Agilent Technologies, Santa Clara, CA). Target primer set sequences were acquired from the PrimerBank database or were designed using GenScript Real-time PCR primer design software (supplementary material Table S1). RNA (1 μg) was reverse transcribed using a High Capacity cDNA Reverse Transcription Kit (Applied Biosystems, Foster City, CA). Quantitative RT-PCR (qPCR) was performed in duplicate, using SYBR green (Qiagen, Hilden, Germany) and a Mx3000P (Agilent). qPCR was performed using the following cycling conditions: 95℃ for 10 min, followed by 40 cycles each consisting of 95℃ for 15 s, 55℃ or 60℃ for 30 s and 72℃ for 30 s. The relative abundance of specific mRNAs was calculated by normalization to the levels of the gene encoding glyceraldehyde-3-phosphate dehydrogenase.

Oil Red O staining and triglyceride measurement

Oil Red O staining was performed as described previously (Wu et al., 1998). The medium was removed from differentiated cells, 10% formalin was added and the cells were incubated for 5 min at room temperature. The formalin was replaced with fresh 10% formalin and incubated for another 2 h at room temperature. Cells were washed well with 60% isopropanol and were incubated with Oil Red O working solution (0.35% Oil Red O in isopropanol:double-distilled water at a ratio of 6:4, mixed immediately before use) for 10 min. The working solution was then washed out with water. Triglyceride levels were measured using a Serum Triglyceride Determination Kit (Sigma-Aldrich, St Louis, MO) according to the manufacturer's instructions.

Culture and differentiation of cells

3T3-L1 and MEF cells were cultured in high-glucose (4500 mg/l) DMEM supplemented with 10% fetal bovine serum (DMEM medium). Differentiation of 3T3L1 preadipocytes was performed as described previously (Frost and Lane, 1985; Green and Kehinde, 1974; Zebisch et al., 2012). For 3T3-L1 adipocyte differentiation, cells were maintained

for the indicated number of days post-confluency and the medium was changed to DMEM containing 0.25 mM IBMX (Wako Pure Chemical Industries), 1.0 µM dexamethasone (Sigma-Aldrich) and 5.0 µg/ml human insulin (Sigma-Aldrich). The cells were incubated in this medium for 2 days. The medium was then replaced by DMEM medium containing only 5.0 µg/ml human insulin, and the cells were maintained in this medium throughout adipocyte differentiation. For differentiation of 3T3-L1 cells that were to be used for electroporation, cells were differentiated at day 0 post-confluency, so that the effect of *AIMP1*-knockdown would last longer. The method used for differentiation of MEFs was the same as that used for differentiation of 3T3-L1 cells, except that the culture medium was supplemented with 0.1 µM rosiglitazone (Cayman) throughout differentiation.

Measurement of AIMP1 and adiponectin in the culture medium

For the measurement of AIMP1 and adiponectin, cell culture medium was harvested at the indicated day and clarified by centrifugation at 4000 ***g*** for 15 min. The levels of AIMP1 and adiponectin in the medium were measured using ELISA kits (Neomics) according to the manufacturer's instructions.

Fractionation of cytoplasm and nucleus

Cells were harvested, washed with ice-cold PBS and lysed with lysis reagent. Cell lysates were centrifuged for 10 min at 800 ***g*** to obtain the nuclear fraction, and the supernatants were collected and centrifuged at 20,000 ***g*** for 15 min to obtain a nuclei-free cytosolic fraction.

Western blotting

Cells were lysed with RIPA buffer (1% NP-40, 1% sodium deoxycholate, 0.1% SDS, 150 mM NaCl, 50 mM Tris pH 7.4, 2 mM EDTA and 50 mM NaF) and incubated on ice for 30 min. The lysates were centrifuged for 20 min at 20,000 ***g***. Supernatants were quantified by using the bicinchoninic acid (BCA) assay and boiled with 5× Laemmli sample buffer. The samples were separated by SDS-PAGE and transferred to PVDF membrane. Proteins were detected using rabbit polyclonal antibodies against AIMP1, PPARγ (sc-7273; Santa Cruz Biotechnology, Dallas, TX), RXRα (sc-553; Santa Cruz Biotechnology), C/EBPα (sc-61; Santa Cruz Biotechnology), aP2 (sc-18661; Santa Cruz Biotechnology), c-jun (sc-45-G; Santa Cruz Biotechnology), c-fos (sc-52; Santa Cruz Biotechnology), γ-tubulin (T6557, Sigma-Aldrich) and GFP (ab6556, Abcam, Cambridge, UK).

Separation of stromal vascular fractions and adipocyte fractions in mice

C57BL/6 mouse embryos and animals at postnatal days 0, 2 and 4 were minced in PBS with calcium chloride and 0.5% bovine serum albumin (BSA). Tissue suspensions were centrifuged at 500 ***g*** for 5 min to remove erythrocytes and free leukocytes. Collagenase type II (Gibco; Invitrogen, Carlsbad, CA) was added to a concentration of 1 mg/ml in DMEM, and the samples were incubated at 37℃ for 20 min with shaking. The cell suspensions were filtered through an 80-µm filter (BD Bioscience) and then spun at 300 ***g*** for 5 min to separate floating adipocytes from the stromal vascular fraction (SVF) pellet. To ensure proper isolation, adipocyte fractions were examined by microscopy before and after plating on plastic to detect adherent cells. Total RNA was isolated from cells by using the RNeasy kit (Qiagen, Hilden, Germany) (Birsoy et al., 2011).

RT-PCR

RNA was extracted according to the protocols of the RNeasy kit (Qiagen). RNA was reverse transcribed with M-MLV reverse transcriptase (Invitrogen) and the cDNA was amplified by PCR and electrophoresed on ethidium-bromide-containing agarose gels. Primers used for PCR were as follows: PPARγ forward, 5′-CTGGTTTCATTAACCTTGATTTG-3′; PPARγ reverse, 5′-ACAAGTCCTTGTAGATCTCCTG-3′; AIMP1 forward, 5′-CAGCAGTCGGCAGCAGCAAGTAC-3′; AIMP1 reverse, 5′-CACACTCAGCATTGGTGTGCAGG-3′; GAPDH forward, 5′-GTGAAGGTCGGTGTGAACGGA-3′; GAPDH reverse, 5′-CCCATCACAAACATGGGGGCA-3′.

Plasmids and transfection

Mouse *AIMP1* cDNA was amplified from 3T3-L1 cells, digested with *Eco*RI and *Sal*I enzymes, and cloned into a pcDNA3 vector (pcDNA3-mAIMP1). Human *AIMP1* was amplified with a Myc-tag encoding primer and cloned into pcDNA3 vector (myc-AIMP1), and the native form of human *AIMP1* was amplified and cloned into a pGEX-4T1 vector (GST-AIMP1). pcDNA3-PPARγ2, PPREx3TK-Luc and GST-PPARγ2 vectors were kindly provided by Chan Soo Shin (Seoul National University, Seoul, Korea) and the GFP-PPARγ vector was kindly provided by Frank J. Gonzalez (National Cancer Institute, Bethesda, MD). All transfection experiments were performed in the 3T3-L1 cell line, using electroporation (Neon, Invitrogen) according to the manufacturer's protocol. Voltage, pulse width and pulse number for electroporation were adjusted to 2500 V, 9 ms and 1, respectively, for the 3T3-L1 cell line. For the *AIMP1*-knockdown experiment, duplex RNAs were synthesized (Invitrogen; sequence, 5′-AACAAUACAACCAAUUCGAAGAUCC-3′) and transfected into cells by electroporation as described above. Stealth™ RNAi Negative Control Duplexes (Invitrogen) were used as the control.

Site-directed mutagenesis

AIMP1 mutants were generated by site-directed mutagenesis using manual methods. The mutants were confirmed by DNA sequencing. The following primers were used to generate the mutant. AIMP1 (KKK267-269AAA) forward, 5′-TCAGGCTGGATCTGCTCCCAAATCGCCGCCGCAGGATTCAGCTCCTTGTCAGGCTC-3′; AIMP1 (KKK267-269AAA) reverse, 5′-GAGCCTGACAAGGAGCTGAATCCTGCGGCGGCGATTTGGGAGCAGATCCAGCCTGA-3′.

Luciferase assay

3T3-L1 cells were transfected with PPREx3TK-Luc, pcDNA3-PPARγ2 and with increasing amounts of pcDNA3-mAIMP1. At 24 h after transfection, cells were lysed with Cell Culture Lysis Reagent (Promega, Madison, WI), incubated for 30 min at 4℃ and centrifuged for 1 min at 20,000 ***g***. Supernatants were transferred to a luminometer plate and luciferase activities were measured according to the manufacturer's protocol (LB96V MicroLumat Plus; EG&G). All experiments were performed in triplicate, and differences in transfection efficiency were compensated for by normalizing the luciferase activity to the β-galactosidase activity.

GST pulldown and immunoprecipitation

GST, GST–AIMP1 and GST–PPARγ2 proteins were purified as follows. Each vector was transformed into Rosetta cells and cultured in Luria broth (LB) medium. Protein expression was induced by 0.5 mM IPTG, and cells were cultured at 18℃ for 9 h. Cells were pelleted, resuspended in protein lysis buffer (50 mM Tris pH 7.4, 120 mM NaCl, 1 mM $MgCl_2$, 1 mM $CaCl_2$, 1 mM EDTA, 1% Triton X-100 and 100 µg/ml PMSF) and sonicated. Cell lysates were centrifuged for 20 min at 20,000 ***g***, and the supernatants were mixed with Glutathione Sepharose™ 4B (GE Healthcare, Little Chalfont, UK) beads and rotated for 6 h at 4℃ in order to bind proteins to the beads. Differentiated 3T3-L1 cells were harvested in 0.1% NP-40 PBS buffer with 100 µg/ml PMSF and sonicated for two rounds of three pulses each at 20% power output and a 50% duty cycle, using a Branson Sonifier 450. The 3T3-L1 lysates and protein-conjugated beads were mixed, and the samples then rotated for 6 h at 4℃. Proteins were pelleted with the beads by centrifugation and were then detected by western blotting. Immunoprecipitation of proteins obtained from transiently transfected cells was performed in the same way as the GST pulldown assay, except that IgG or anti-Myc antibodies (sc-40; Santa Cruz Biotechnology) were conjugated to Protein-G–agarose beads (Invitrogen).

Electrophoretic mobility shift assay

Electrophoretic mobility shift assay (EMSA) was performed using an EMSA Gel-Shift kit (Panomics, Fremont, CA) according to the manufacturer's protocol. Briefly, eluted GST or GST–AIMP1 proteins were incubated with differentiated 3T3-L1 nuclear extracts, binding buffer, poly d(I-C) and a biotin-labeled PPRE probe, before being

separated by SDS-PAGE. 3T3-L1 nuclear extract was prepared by disruption and centrifugation of 3T3-L1 cells in 0.5% NP-40-sucrose buffer. An unlabeled PPRE probe was used as the cold probe. Probe signals were detected by western blotting using a streptavidin–horseradish-peroxidase conjugate.

Preparation of recombinant adenovirus

Recombinant adenovirus containing human *AIMP1* cDNA was constructed using an Adenoviral Expression Kit (Clontech, Mountain View, CA). Recombinant adenovirus bearing the bacterial β-galactosidase gene (Adv-LacZ) was used as control.

Animals and *in vivo* adenovirus injection into the fat pad

Animal studies were conducted in accordance with the institutional guidelines for animal experiments of Seoul National University. Male C57BL/6 mice were housed individually and high-fat-chow feeding (32% safflower oil, 33.1% casein, 17.6% sucrose and 5.6% cellulose) was initiated at 5 weeks of age. After 4 weeks of high-fat-chow loading, body-weight-matched mice were anesthetized prior to dissection of the skin and body wall. An adenoviral preparation (1×10^8 plaque-forming units in a volume of 20 µl) was injected at two points on each side of the epididymal fat pad and the subcutaneous fat tissues in the flank, i.e. each mouse was injected at a total of four points (Yamada et al., 2006).

Blood analysis

Blood AIMP1, serum insulin, adiponectin, TNFα, triglyceride and NEFA levels were determined as described previously (Park et al., 2006).

Intraperitoneal gluocose-tolerance test

IPGTTs were performed on fasted (10 h, daytime) mice. Mice were given glucose (2 g/kg of body weight) intraperitoneally, followed by measurement of blood glucose levels.

Acknowledgements

We thank the members of the Medicinal Bioconvergence Research Center (Seoul National University) for reagents and for helpful discussions.

Competing interests

The authors declare no competing interests.

Author contributions

J.H.K. wrote the paper, performed the experiments and analyzed the data. J.H.L., M.C.P., I.Y., K.K. and M.L. performed experiments. H.-S.C. analyzed the data. J.M.H. performed experiments, analyzed data and wrote the paper. S.K. conceived of the project. All authors contributed to discussion.

Funding

This work was supported by the Global Frontier Project [grant numbers NRF-M3A6A4-2010-0029785 and NRF-M3A6A4072536]; by the Basic Science Research Program [grant number 2012R1A1A2040060] of the National Research Foundation]; by the Ministry of Science, ICT and Future Planning (MSIP) of Korea; and by the Yonsei University Global Specialization Project of 2014.

Supplementary material

Supplementary material available online at
http://jcs.biologists.org/lookup/suppl/doi:10.1242/jcs.154930/-/DC1

References

Birsoy, K., Berry, R., Wang, T., Ceyhan, O., Tavazoie, S., Friedman, J. M. and Rodeheffer, M. S. (2011). Analysis of gene networks in white adipose tissue development reveals a role for ETS2 in adipogenesis. *Development* **138**, 4709-4719.

Çirakoğlu, B., Mirande, M. and Waller, J. P. (1985). A model for the structural organization of aminoacyl-tRNA synthetases in mammalian cells. *FEBS Lett.* **183**, 191-194.

Cohen, R. N. (2006). Nuclear receptor corepressors and PPARgamma. *Nucl. Recept. Signal.* **4**, e003.

Cohen, R. N., Wondisford, F. E. and Hollenberg, A. N. (1998). Two separate NCoR (nuclear receptor corepressor) interaction domains mediate corepressor action on thyroid hormone response elements. *Mol. Endocrinol.* **12**, 1567-1581.

Couture, J. P., Daviau, A., Fradette, J. and Blouin, R. (2009). The mixed-lineage kinase DLK is a key regulator of 3T3-L1 adipocyte differentiation. *PLoS ONE* **4**, e4743.

Frost, S. C. and Lane, M. D. (1985). Evidence for the involvement of vicinal sulfhydryl groups in insulin-activated hexose transport by 3T3-L1 adipocytes. *J. Biol. Chem.* **260**, 2646-2652.

Galic, S., Oakhill, J. S. and Steinberg, G. R. (2010). Adipose tissue as an endocrine organ. *Mol. Cell. Endocrinol.* **316**, 129-139.

Gao, Y., Koppen, A., Rakhshandehroo, M., Tasdelen, I., van de Graaf, S. F., van Loosdregt, J., van Beekum, O., Hamers, N., van Leenen, D., Berkers, C. R. et al. (2013). Early adipogenesis is regulated through USP7-mediated deubiquitination of the histone acetyltransferase TIP60. *Nat. Commun.* **4**, 2656.

Gavrilova, O., Haluzik, M., Matsusue, K., Cutson, J. J., Johnson, L., Dietz, K. R., Nicol, C. J., Vinson, C., Gonzalez, F. J. and Reitman, M. L. (2003). Liver peroxisome proliferator-activated receptor gamma contributes to hepatic steatosis, triglyceride clearance, and regulation of body fat mass. *J. Biol. Chem.* **278**, 34268-34276.

Green, H. and Kehinde, O. (1974). Sublines of mouse 3T3 cells that accumulate lipid. *Cell* **1**, 113-116.

Grimaldi, P. A. (2001). The roles of PPARs in adipocyte differentiation. *Prog. Lipid Res.* **40**, 269-281.

Han, J. M., Lee, M. J., Park, S. G., Lee, S. H., Razin, E., Choi, E. C. and Kim, S. (2006). Hierarchical network between the components of the multi-tRNA synthetase complex: implications for complex formation. *J. Biol. Chem.* **281**, 38663-38667.

Han, J. M., Park, S. G., Liu, B., Park, B. J., Kim, J. Y., Jin, C. H., Song, Y. W., Li, Z. and Kim, S. (2007). Aminoacyl-tRNA synthetase-interacting multifunctional protein 1/p43 controls endoplasmic reticulum retention of heat shock protein gp96: its pathological implications in lupus-like autoimmune diseases. *Am. J. Pathol.* **170**, 2042-2054.

Han, J. M., Myung, H. and Kim, S. (2010). Antitumor activity and pharmacokinetic properties of ARS-interacting multi-functional protein 1 (AIMP1/p43). *Cancer Lett.* **287**, 157-164.

Han, R., Kitlinska, J. B., Munday, W. R., Gallicano, G. I. and Zukowska, Z. (2012). Stress hormone epinephrine enhances adipogenesis in murine embryonic stem cells by up-regulating the neuropeptide Y system. *PLoS ONE* **7**, e36609.

Haque, W. A. and Garg, A. (2004). Adipocyte biology and adipocytokines. *Clin. Lab. Med.* **24**, 217-234.

Jing, E., Gesta, S. and Kahn, C. R. (2007). SIRT2 regulates adipocyte differentiation through FoxO1 acetylation/deacetylation. *Cell Metab.* **6**, 105-114.

Kalra, P. S. and Kalra, S. P. (2002). Obesity and metabolic syndrome: long-term benefits of central leptin gene therapy. *Drugs Today (Barc)* **38**, 745-757.

Kim, J. B., Wright, H. M., Wright, M. and Spiegelman, B. M. (1998). ADD1/SREBP1 activates PPARgamma through the production of endogenous ligand. *Proc. Natl. Acad. Sci. USA* **95**, 4333-4337.

Kim, S., You, S. and Hwang, D. (2011). Aminoacyl-tRNA synthetases and tumorigenesis: more than housekeeping. *Nat. Rev. Cancer* **11**, 708-718.

Koppen, A. and Kalkhoven, E. (2010). Brown vs white adipocytes: the PPARgamma coregulator story. *FEBS Lett.* **584**, 3250-3259.

Kubo, M., Ijichi, N., Ikeda, K., Horie-Inoue, K., Takeda, S. and Inoue, S. (2009). Modulation of adipogenesis-related gene expression by estrogen-related receptor gamma during adipocytic differentiation. *Biochim. Biophys. Acta* **1789**, 71-77.

Lee, S. W., Cho, B. H., Park, S. G. and Kim, S. (2004). Aminoacyl-tRNA synthetase complexes: beyond translation. *J. Cell Sci.* **117**, 3725-3734.

Lefterova, M. I., Zhang, Y., Steger, D. J., Schupp, M., Schug, J., Cristancho, A., Feng, D., Zhuo, D., Stoeckert, C. J., Jr, Liu, X. S. et al. (2008). PPARgamma and C/EBP factors orchestrate adipocyte biology via adjacent binding on a genome-wide scale. *Genes Dev.* **22**, 2941-2952.

Méndez-Sánchez, N., Chavez-Tapia, N. C., Zamora-Valdés, D. and Uribe, M. (2006). Adiponectin, structure, function and pathophysiological implications in non-alcoholic fatty liver disease. *Mini Rev. Med. Chem.* **6**, 651-656.

Mirande, M., Gache, Y., Le Corre, D. and Waller, J. P. (1982). Seven mammalian aminoacyl-tRNA synthetases co-purified as high molecular weight entities are associated within the same complex. *EMBO J.* **1**, 733-736.

Norcum, M. T. (1989). Isolation and electron microscopic characterization of the high molecular mass aminoacyl-tRNA synthetase complex from murine erythroleukemia cells. *J. Biol. Chem.* **264**, 15043-15051.

Ntambi, J. M. and Young-Cheul, K. (2000). Adipocyte differentiation and gene expression. *J. Nutr.* **130**, 3122S-3126S.

Park, S. G., Jung, K. H., Lee, J. S., Jo, Y. J., Motegi, H., Kim, S. and Shiba, K. (1999). Precursor of pro-apoptotic cytokine modulates aminoacylation activity of tRNA synthetase. *J. Biol. Chem.* **274**, 16673-16676.

Park, H., Park, S. G., Kim, J., Ko, Y. G. and Kim, S. (2002a). Signaling pathways for TNF production induced by human aminoacyl-tRNA synthetase-associating factor, p43. *Cytokine* **20**, 148-153.

Park, S. G., Kang, Y. S., Ahn, Y. H., Lee, S. H., Kim, K. R., Kim, K. W., Koh, G. Y., Ko, Y. G. and Kim, S. (2002b). Dose-dependent biphasic activity of tRNA synthetase-associating factor, p43, in angiogenesis. *J. Biol. Chem.* **277**, 45243-45248.

Park, S. G., Shin, H., Shin, Y. K., Lee, Y., Choi, E. C., Park, B. J. and Kim, S. (2005). The novel cytokine p43 stimulates dermal fibroblast proliferation and wound repair. *Am. J. Pathol.* **166**, 387-398.

Park, S. G., Kang, Y. S., Kim, J. Y., Lee, C. S., Ko, Y. G., Lee, W. J., Lee, K. U., Yeom, Y. I. and Kim, S. (2006). Hormonal activity of AIMP1/p43 for glucose homeostasis. *Proc. Natl. Acad. Sci. USA* **103**, 14913-14918.

Park, S. G., Schimmel, P. and Kim, S. (2008). Aminoacyl tRNA synthetases and their connections to disease. *Proc. Natl. Acad. Sci. USA* **105**, 11043-11049.

Picard, F., Kurtev, M., Chung, N., Topark-Ngarm, A., Senawong, T., Machado De Oliveira, R., Leid, M., McBurney, M. W. and Guarente, L. (2004). Sirt1 promotes fat mobilization in white adipocytes by repressing PPAR-gamma. *Nature* **429**, 771-776.

Quevillon, S. and Mirande, M. (1996). The p18 component of the multisynthetase complex shares a protein motif with the beta and gamma subunits of eukaryotic elongation factor 1. *FEBS Lett.* **395**, 63-67.

Quevillon, S., Agou, F., Robinson, J. C. and Mirande, M. (1997). The p43 component of the mammalian multi-synthetase complex is likely to be the precursor of the endothelial monocyte-activating polypeptide II cytokine. *J. Biol. Chem.* **272**, 32573-32579.

Quevillon, S., Robinson, J.-C., Berthonneau, E., Siatecka, M. and Mirande, M. (1999). Macromolecular assemblage of aminoacyl-tRNA synthetases: identification of protein-protein interactions and characterization of a core protein. *J. Mol. Biol.* **285**, 183-195.

Rosen, E. D. and Spiegelman, B. M. (2006). Adipocytes as regulators of energy balance and glucose homeostasis. *Nature* **444**, 847-853.

Rosen, E. D., Sarraf, P., Troy, A. E., Bradwin, G., Moore, K., Milstone, D. S., Spiegelman, B. M. and Mortensen, R. M. (1999). PPAR gamma is required for the differentiation of adipose tissue in vivo and in vitro. *Mol. Cell* **4**, 611-617.

Rosen, E. D., Walkey, C. J., Puigserver, P. and Spiegelman, B. M. (2000). Transcriptional regulation of adipogenesis. *Genes Dev.* **14**, 1293-1307.

Spiegelman, B. M. (1998). PPAR-gamma: adipogenic regulator and thiazolidinedione receptor. *Diabetes* **47**, 507-514.

Tang, Q. Q., Otto, T. C. and Lane, M. D. (2003). Mitotic clonal expansion: a synchronous process required for adipogenesis. *Proc. Natl. Acad. Sci. USA* **100**, 44-49.

Tontonoz, P. and Spiegelman, B. M. (2008). Fat and beyond: the diverse biology of PPARgamma. *Annu. Rev. Biochem.* **77**, 289-312.

Tontonoz, P., Hu, E. and Spiegelman, B. M. (1994). Stimulation of adipogenesis in fibroblasts by PPAR gamma 2, a lipid-activated transcription factor. *Cell* **79**, 1147-1156.

Trayhurn, P. and Beattie, J. H. (2001). Physiological role of adipose tissue: white adipose tissue as an endocrine and secretory organ. *Proc. Nutr. Soc.* **60**, 329-339.

Wang, F. and Tong, Q. (2009). SIRT2 suppresses adipocyte differentiation by deacetylating FOXO1 and enhancing FOXO1's repressive interaction with PPARgamma. *Mol. Biol. Cell* **20**, 801-808.

Wu, Z., Xie, Y., Morrison, R. F., Bucher, N. L. and Farmer, S. R. (1998). PPARgamma induces the insulin-dependent glucose transporter GLUT4 in the absence of C/EBPalpha during the conversion of 3T3 fibroblasts into adipocytes. *J. Clin. Invest.* **101**, 22-32.

Yamada, T., Katagiri, H., Ishigaki, Y., Ogihara, T., Imai, J., Uno, K., Hasegawa, Y., Gao, J., Ishihara, H., Niijima, A. et al. (2006). Signals from intra-abdominal fat modulate insulin and leptin sensitivity through different mechanisms: neuronal involvement in food-intake regulation. *Cell Metab.* **3**, 223-229.

Yu, S., Matsusue, K., Kashireddy, P., Cao, W. Q., Yeldandi, V., Yeldandi, A. V., Rao, M. S., Gonzalez, F. J. and Reddy, J. K. (2003). Adipocyte-specific gene expression and adipogenic steatosis in the mouse liver due to peroxisome proliferator-activated receptor gamma1 (PPARgamma1) overexpression. *J. Biol. Chem.* **278**, 498-505.

Yu, C., Markan, K., Temple, K. A., Deplewski, D., Brady, M. J. and Cohen, R. N. (2005). The nuclear receptor corepressors NCoR and SMRT decrease peroxisome proliferator-activated receptor gamma transcriptional activity and repress 3T3-L1 adipogenesis. *J. Biol. Chem.* **280**, 13600-13605.

Zebisch, K., Voigt, V., Wabitsch, M. and Brandsch, M. (2012). Protocol for effective differentiation of 3T3-L1 cells to adipocytes. *Anal. Biochem.* **425**, 88-90.

Supplemental material Fig. 1. AIMP1 had no effect on SREBP1c or ERRγ transcriptional activity.

A. HEK293 cells were transfected with the indicated plasmids, viz., SREBP1c, AIMP1, and a reporter plasmid, viz. the SREBP1c-response element-luciferase (SRE-Luc). After transfection, cells were harvested for the luciferase assays. Luciferase activity was normalized to β-gal activity. **B**. HEK293 cells were transfected with the indicated plasmids, namely ERRγ, AIMP1, and a reporter plasmid, ERRγ-response element-luciferase (ERE-Luc). After transfection, cells were harvested for luciferase assays. Luciferase activity was normalized to β-gal activity. Data are presented as means and S.D. **C**. HEK293 cells were transfected with the indicated plasmids. After transfection, cells were harvested for the luciferase assays. Luciferase activity was normalized to β-gal activity.

Supplementary Table. 1. Specific primers for quantitative RT-PCR

A

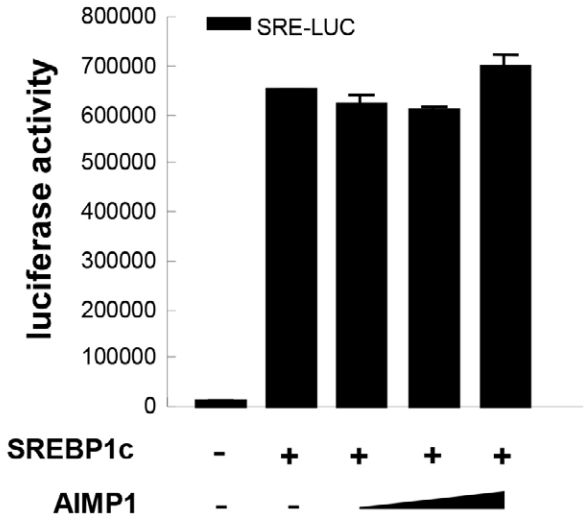
SRE-LUC
luciferase activity
800000
700000
600000
500000
400000
300000
200000
100000
0
SREBP1c - + + + +
AIMP1 - - ▲

B

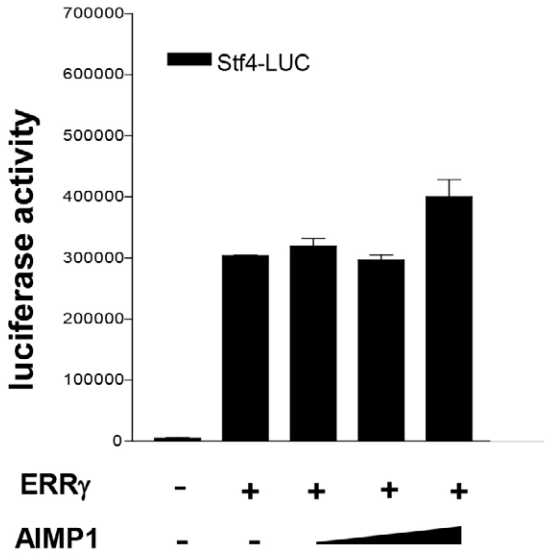
Stf4-LUC
luciferase activity
700000
600000
500000
400000
300000
200000
100000
0
ERRγ - + + + +
AIMP1 - - ▲

C

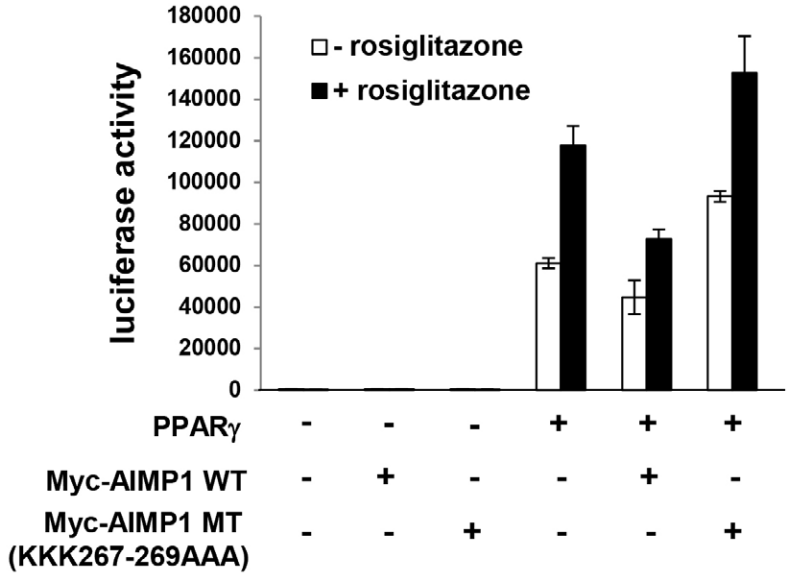
□- rosiglitazone
■+ rosiglitazone
luciferase activity
180000
160000
140000
120000
100000
80000
60000
40000
20000
0
PPARγ - - - + + +
Myc-AIMP1 WT - + - - + -
Myc-AIMP1 MT (KKK267-269AAA) - - + - - +

Supplemental Table 1. Primer sets used in quantitative RT-PCR analysis

No.	Gene Symbol	Gene name	Gene Accession #	Forward (5'-->3')	Reverse (5'-->3')	size (bp)	Annealting temp (°C)
1	AIMP1	aminoacyl tRNA synthetase complex-interacting multifunctional protein 1	NM_007926.2	TTTCTCTGCCGATTCTGGGGA	CCTGCTGCTTGAGATATTCGAT	109	55
2	AIMP2	aminoacyl tRNA synthase complex-interacting multifunctional protein 2 isoform 1	NM_001172146.1	CGT GCA GGA AAC ATC CGA	GTT ACG TCC AAG TCT GCA TCT	153	55
3	AIMP3	aminoacyl tRNA synthase complex-interacting multifunctional protein 3	NM_025380.2	GACTGAAGCCGGGGAATAAGT	TAGACTCGGGCCATTGTTTGT	80	55
4	EPRS	glutamyl-prolyl-tRNA synthetase	NM_029735.1	TGCGCTACCTGGCTAGAATTG	GCCTATCACACGAAGACAACTTT	120	55
5	LRS	leucyl-tRNA synthetase	NM_134137.2	CATTTGGGACACACGTTTTCC	GCATACCAGTACAGTGCAACC	109	55
6	IRS	isoleucine-tRNA synthetase	NM_172015.3	CCTCCCTTTGCTACTGGACTG	TCTTCTGTCAACGTGAAACCC	108	55
7	MRS	methionyl tRNA syntethease	NM_001171582.1	TACCATTCCTTACCCGGCCTA	GCAGATTGCACTAGCAGAGAA	80	55
8	DRS	aspartate--tRNA ligase, cytoplasmic isoform 1	NM_177445.5	CAGCAGTTTAATGTCCAGGCT	GCCGAATGGCATCATCCAG	238	60
9	RRS	arginyl-tRNA synthetase	NM_025936.3	GACAAAGTTGAAATTGCGGGTC	GAGACTGGTTAGCTGTTCTGAC	81	55
10	VRS	valyl-tRNA synthetase	NM_011690.3	GGCCAGGTCTGTCACTCAAC	TTTCTCCCGTTTCTTTGCCTC	94	60
11	WRS	tryptophanyl-tRNA synthetase	NM_011710.3	CTTCAACCAAGTGAAAGGCA	GATCTTCGGGAAAGAGTTGC	112	55
12	HRS	histidyl-tRNA synthetase	NM_008214.4	GAGGAGCTGGTACGACTCCA	GGCGTTTGAAACAGCGGATG	238	60
13	Sirt1	sirtuin 1	NM_019812.2	CAGCATCTTGCCTGATTTGT	GCACCGAGGAACTACCTGAT	83	55
14	PPARgamma1	peroxisome proliferator-activated receptor gamma isoform 1	NM_001127330.1	GGAAGACCACTCGCATTCCTT	GTAATCAGCAACCATTGGGTCA	121	55
15	PPARgamma2	peroxisome proliferator-activated receptor gamma isoform 2	NM_011146.3	TCGCTGATGCACTGCCTATG	GAGAGGTCCACAGAGCTGATT	103	55
16	aP2	fatty acid binding protein 4, adipocyte	NM_024406.2	AAGGTGAAGAGCATCATAACCCT	TCACGCCTTTCATAACACATTCC	133	55
17	LPL	lipoprotein lipase	NM_008509.2	GGGAGTTTGGCTCCAGAGTTT	TGTGTCTTCAGGGGTCCTTAG	115	55
18	C/EBPalpha	CCAAT/enhancer binding protein (C/EBP), alpha	NM_007678.3	CAAGAACAGCAACGAGTACCG	GTCACTGGTCAACTCCAGCAC	124	55
19	GAPDH	glyceraldehyde-3-phosphate dehydrogenase	NM_008084.2	AGGTCGGTGTGAACGGATTTG	GGGGTCGTTGATGGCAACA	95	55